Progress in Neuropsychopharmacology & Biological Psychiatry 104 (2021) 110026

Contents lists available at ScienceDirect

Progress in Neuropsychopharmacology & Biological Psychiatry

journal homepage: www.elsevier.com/locate/pnp

Frequency-specific alteration of functional connectivity density in bipolar disorder depression

Yang Yang[a], Qian Cui[b,*], Yajing Pang[a], Yuyan Chen[a], Qin Tang[a], Xiaonan Guo[a], Shaoqiang Han[a], Ahmed Ameen Fateh[a], Fengmei Lu[a], Zongling He[a], Jing Huang[a], Ailing Xie[b], Di Li[a], Ting Lei[b], Yifeng Wang[a], Huafu Chen[a,c,d,e,*]

[a] The Clinical Hospital of Chengdu Brain Science Institute, School of Life Science and Technology, University of Electronic Science and Technology of China, Chengdu, China
[b] School of Public Affairs and Administration, University of Electronic Science and Technology of China, Chengdu, China
[c] MOE Key Lab for Neuroinformation, University of Electronic Science and Technology of China, Chengdu, China
[d] High-Field Magnetic Resonance Brain Imaging Key Laboratory of Sichuan Province, University of Electronic Science and Technology of China, Chengdu, China
[e] Department of Radiology, First Affiliated Hospital to Army Medical University, Chongqing, China

ARTICLE INFO

Keywords:
Bipolar disorder
Depression
Functional connectivity density
Slow-5
Slow-4

ABSTRACT

Functional dysconnectivity has been widely reported in bipolar disorder during depressive episodes (BDD). However, the frequency-specific alterations of functional connectivity (FC) in BDD remain poorly understood. To address this issue, the FC patterns across slow-5 (0.01–0.027 Hz) and slow-4 (0.027–0.073 Hz) bands were computed using resting-state functional magnetic resonance imaging data from 37 BDD patients and 56 healthy controls (HCs). Short-range (local) FC density (lfcd) and long-range FC density (lrfcd) were calculated, and two-way analysis of variance was performed to ascertain the main effect of diagnosis and interaction effects between diagnosis and frequency. The BDD patients showed increased lfcd in the midline cerebelum. Meanwhile, the BDD patients showed increased lrfcd in the left supplementary motor cortex and right striatum and decreased lrfcd in the bilateral inferior temporal gyrus and left angular gyrus (AG) compared with the HCs. A significant frequency-by-diagnosis interaction was observed. In the slow-4 band, the BDD patients showed increased lfcd in the left pre-/postcentral gyrus and left fusiform gyrus (FG) and increased lrfcd in the left lingual gyrus (LG). In the slow-5 band, the BDD patients showed decreased lrfcd in the left LG. Moreover, the increased lfcd in the left FG in the slow-4 band was correlated with clinical progression and decreased lrfcd in the left AG was correlated with depressive severity. These results suggest that the presence of aberrant communication in the default mode network, sensory network, and subcortical and limbic modulating regions (striatum and midline cerebelum), which may offer a new framework for the understanding of the pathophysiological mechanisms of BDD.

1. Introduction

Depressive episodes are the most common mood manifestations of bipolar disorder (BD) (Mitchell and Malhi, 2004), devastating patients' social life and the basic acts of self-care (Mitchell et al., 2010). BD patients in depressive episodes (BDD) experience feelings of worthlessness, negative mood, anhedonia, rumination, and psychomotor retardation (Grande et al., 2016). Previous neuroimaging studies have advanced our understanding of the neural mechanism of BDD. In contrast to the single-brain region, BDD patients have a tendency to dysfunction in the neural circuits related to sensory, affect, thought, reward, and cognitive control (Perry et al., 2018; Satterthwaite et al., 2015; Spielberg et al., 2016).

Resting-state functional connectivity analysis (FC) is an effective method to investigate the intrinsic temporally coherent brain networks (Smith et al., 2009). Based on a seed-based approach, abnormal FC patterns in the cortical-limbic (Anand et al., 2009; Magioncalda et al., 2015), insular-sensory (Pang et al., 2018), and fronto-insular (Ambrosi et al., 2017) circuits were found in the BDD patients relative to healthy controls (HCs). Independent component analysis of BDD patients demonstrated that, increased FC within the frontoparietal network (Goya-Maldonado et al., 2016) and increased FC between cognitive control and sensorimotor network (SMN) (He et al., 2016). The impairments in cognitive networks may reflect the impaired top-down control in emotional processing in BDD. Moreover, the graph theory analysis of whole-brain FC study has revealed a greater local efficiency in the

* Corresponding authors at: School of Life Science and Technology, University of Electronic Science and Technology of China, Chengdu, China (H.Chen).
E-mail addresses: qiancui26@gmail.com (Q. Cui), chenhf@uestc.edu.cn (H. Chen).

https://doi.org/10.1016/j.pnpbp.2020.110026
Received 16 July 2019; Received in revised form 31 May 2020; Accepted 21 June 2020
Available online 02 July 2020

default mode network (DMN) in BDD (He et al., 2016). Despite the intriguing findings, previous FC studies limited the potential to fully assess the functional properties of brain connectomics due to their reliance on specific regions or networks. Voxel-wise FC density (fcd) mapping is a powerful method for describing whole-brain FC pattern through the calculation of short-range (local) FC density (lfcd) and long-range FC density (lrfcd) (Guo et al., 2020; Tomasi and Volkow, 2010, 2012). Lfcd refers to the count of FCs between a given voxel and its local cluster, whereas lrfcd refers to the count of FCs between a voxel and remote voxels. The efficient and well-organized functioning of the human brain depends on local and long-range connections (Shuixia et al., 2014). Using the fcd method, Wang and his colleagues (Wang et al., 2017b, 2016) found disrupted intrinsic FC in the DMN and limbic system in BDD patients.

However, the above mentioned findings were based on spontaneous low frequency (0.01–0.1 Hz) oscillations, which overlapped with multiple frequency bands, such as slow-5 (0.01–0.027 Hz), slow-4 (0.027–0.073 Hz), and part of slow-3 (0.073–0.198 Hz) bands (Buzsáki and Draguhn, 2004). These sub-frequency bands were previously defined by an electrophysiological study, high-frequency bands, such as slow-3, are primarily restricted to the white matter (Zuo et al., 2010) and can be affected by physiological variables, such as respiration and aliased cardiac signals (Cordes et al., 2001). The amplitude of low frequency fluctuations in the slow-4 band are high in many brain regions such as the basal ganglia, thalamus, precuneus, and several sensorimotor regions, whereas that of the anterior DMN is high in the slow-5 (Zuo et al., 2010). To the best of our knowledge, only two studies used the frequency-specific methods to investigate the pathomechanisms of BDD. One research used perigenual anterior cingulate cortex (pgACC) as the seed, and the slow-5 specific dysconnectivity between pgACC and supragenual anterior cingulate cortex in BDD group was found (Magioncalda et al., 2015). Another research used the variability method and found that slow-5 specific variance was increased in the DMN but decreased in the SMN in BDD patients (Martino et al., 2016). However, frequency-specific changes in the voxel-level FC among BDD patients have not been investigated.

Accordingly, the present study aimed to investigate the frequency-related changes in lfcd and lrfcd across slow-5 and slow-4 bands among BDD patients. We hypothesized that the location of fcd changes might be frequency-specific in the sensory, affect, and cognitive circuits. We further predicted that the frequency-dependent fcd of aberrant brain regions could be correlated with clinical variables among BDD patients.

2. Materials and methods

2.1. Participants

A total of forty BDD patients were recruited from a mental health center of Chengdu, Sichuan, China. All patients were interviewed by two experienced psychiatrists by using the Structured Clinical Interview for DSM-IV-TR-Patient edition (SCID-P, 2/2001 revision). The exclusion criteria included schizophrenia, mental retardation or personality disorder, history of loss of consciousness, substance abuse, and serious medical or neurological illness. The clinical state of the patients was evaluated using 24-item Hamilton Depression Rating (HAMD) Scale. Other clinical characteristic data, including the age of first onset, number of depressive episodes, number of manic episodes, duration of illness, and total medication load, were collected. The BDD patients were treated with antidepressants, mood stabilizers, and antipsychotics. To measure the total medication load, we used a previously described strategy (Almeida et al., 2009; Amelia, 2008) and converted each antidepressant and mood stabilizer dosage into absent (0), low- (1) or high-dose (2) groups (Sackeim, 2001). Medicines (e.g., escitalopram, duloxetine, and valproate) that were not included by Sackeim were coded as 0, 1, or 2 with reference to the midpoint of the daily dose range recommended by the Physician's Desk-Reference. Then, we converted antipsychotic doses into chlorpromazine dose equivalents coded as 0, 1, or 2 for no medication, below, or above 300 mg/day, respectively, as described by Davis and Chen (John, 2004). Lastly, we calculated the composite measure of total medication load for each patient. Sixty-three HCs who were closely matched in terms of age, sex, handedness, and years of education with BDD patients were recruited through advertisements. The SCID non-patient version was employed to ensure the lifetime absence of psychiatric illnesses among HCs. Written informed consent was obtained from each participant before experimentation. This study was approved by the research ethical committee of the University of Electronic Science and Technology of China.

2.2. fMRI data acquisition

The data of all participants were collected with a 3T GE DISCOVERY MR750 scanner (General Electric, Fairfield Connecticut, USA) equipped with a high-speed gradient and eight-channel prototype quadrature birdcage head coil. Foam pads and headphones were used to minimize head movement and scanner noise. The participants were instructed to rest with their eyes closed and remain motionless, and avoid falling to sleep. The functional images were collected through an echo-planar imaging (EPI) sequence with the following parameters: TR/TE = 2000/30 ms, slices = 43, matrix size = 64 × 64, FA = 90°, FOV = 240 × 240 mm^2, voxel size = 3.75 × 3.75 × 3.2 mm^3, slice thickness = 3.2 mm, no gap, and total of 255 volumes. Thus, the 8.5-min resting state scans were obtained for each participant. The T1 structural image was scanned using the following parameters: TR/TE = 5.92/1.956 ms, slices = 156, matrix size = 256 × 256, FA = 12°, FOV = 256 × 256 mm^2, voxel size = 1 × 1 × 1 mm^3, slice thickness = 1 mm, and no gap.

2.3. Data preprocessing

Data preprocessing was carried out using the DPABI toolbox (http://rfmri.org/dpabi). The first five volumes for each participant were discarded to ensure signal stability, and the remaining volumes were corrected for slice timing and head motion. The data of the participants with head motion parameters that exceeded 2 mm in the x, y, or z directions or 2° rotation of each axis were discarded for further analysis. Three BDD patients and four HCs were excluded on the basis of this criterion. All realigned data were spatially normalized using a unified segmentation of anatomical images and resampled into a voxel size of 3 × 3 × 3 mm^3. Normalization involved the following three steps: 1) T1 structural images of each participant were co-registered to the corresponding functional images; 2) Co-registered T1 images were segmented into gray matter, white matter, and cerebrospinal fluid on the basis of transformation parameters that indicated transformation from subject native space into the standard Montreal Neurological Institute (MNI) space; 3) Functional images were finally transformed into the standard space through the application of transformation parameters. Three HCs were excluded due to lack of the structural scans. Thirty-seven BDD patients and fifty-six HCs were left for the following analyses. We did not apply spatial smoothing to the fMRI images to control the smoothing effect on local correlations (Tomasi and Volkow, 2012). Subsequently, the blood oxygenation level-dependent signal of each voxel was detrended to abandon the linear trend. Several spurious covariates, including head motion parameters (Friston 24-parameter model) (Friston et al., 1996), mean signals from the white matter and cerebrospinal fluid were regressed to reduce the noise signals. Temporal band-pass filtering was then performed in the slow-5 and slow-4 frequency bands. Finally, the "bad" time points were removed from the time series by employing a "scrubbing" cut method with a frame deviation (FD) (Power et al., 2012) threshold of 0.5 mm. The FD across time points was calculated for each participant to examine the confounding influence of head motion on connectivity measures. Mean FD of the BDD group (0.09 ± 0.06) and HCs group (0.09 ± 0.04) was

also nonsignificant ($p = 0.75$) by the two-sample t test. After scrubbing, the remaining time points of the BDD (247 ± 7) and HC groups (248 ± 3) were nonsignificant ($p = 0.18$), as indicated by the two-sample t test. The retaining time points of all participants were > 80% of the original signals after scrubbing and were included for further analysis.

2.4. Functional connectivity density

The lfcd at a given voxel i is the local $l(x_i)$ between i and its neighbor voxels as indicated by the 3D searching algorithm developed in Interactive Data Language (Tomasi and Volkow, 2010). In brief, we initially computed the FC between x_i and each voxel x_j, which was directly neighboring with x_i with an FC greater than T. Next, we calculated the FC between x_i and x_k, which was directly neighboring with x_j but not with x_i, and the FC greater than T was considered as the neighbor of x_i. This search strategy was continued until no further voxels could be included. The global fcd (gfcd) at x_i was calculated as the global number of connections, $g(x_i)$, between x_i and all other voxels in the gray matter mask. FCs with x_i greater than T were considered as functionally connected. Here, the correlation coefficient threshold T was set in accordance with the criterion of $p < 0.05$, family-wise-error corrected. This correlation coefficient threshold was used to reduce the chance of false positive connections across all subjects (Wang et al. (2017a)). In addition, a different correlation coefficient threshold was also used to validate the stability of our results (see detailed information in supplementary material). Lfcd and gfcd were obtained, and we defined lrfcd as gfcd minus lfcd to remove the number of local connections. Subsequently, the lfcd and lrfcd maps were Median-IQR standardization using the DPABI toolbox for each subject. Finally, the lfcd and lrfcd maps were spatially smoothed with full width at half maxima = 6 mm.

2.5. Statistical analysis

Two-way analysis of variance was conducted in the Statistical Parametric Mapping 12 (https://www.fil.ion.ucl.ac.uk/spm/) with the diagnoses (two levels: BDD and HCs) as a between-subject factor, frequency band (two levels: slow-5 and slow-4) as a within-subject factor, and age, years of education, and mean FD as covariates of no interest. Multiple comparison correction for each main and interaction effect was using the Gaussian random field (GRF) method with an individual voxel $p < 0.005$ and a cluster level $p < 0.05$ in the DPABI toolbox. The surviving brain clusters were selected as the regions of interest (ROIs) for the following post-hoc analysis: A two-tailed, two-sample t test was conducted on these main effect ROIs to determine the changes between the diagnoses (BDD and HCs), and the statistical level of $p < 0.05$ was considered as significant. Likewise, this test was conducted on these interaction effect ROIs to determine the changes between the diagnoses (BDD and HCs) in different frequency bands (i.e., slow-4 and slow-5), and the statistical level of $p < 0.05$ was considered as significant.

Correlations between the lfcd and lrfcd of these post-hoc significantly changed ROIs and clinical variables were further detected via correlation analysis with the total medication load as a covariate. Specifically, we calculated the Pearson correlation for numeric variables, while for nominal variable, the Spearman correlation was used.

3. Results

3.1. Demographic characteristics and clinical variables

Demographic characteristics and clinical scores were shown in Table1. No significant difference between BDD group and HCs group was found in terms of age, handedness, sex, and years of education.

Table 1
Characteristics of demographic and clinical variables of HCs and patients with BDD.

Variables	HCs (n = 56)	BDD (n = 37)	p-value
Age (Years)	30.75 ± 9.97	34.19 ± 10.49	0.11[a]
Sex (Male/Female)	30/26	20/17	0.96[b]
Handedness (Left/Right)	1/55	1/36	0.77[b]
Education (Years)	14.45 ± 3.92	13.81 ± 3.03	0.41[a]
Duration of illness (Months)	–	96.86 ± 92.97	–
Age of first onset (Years)	–	26.97 ± 9.01	–
Number of depressive episodes	–	2.57 ± 1.12	–
Number of manic episodes	–	1.65 ± 1.11	–
HAMD score	–	23.05 ± 6.62	–
		Medical	
Medication load index			
Antidepressants, no. of patients			
Fluoxetine		3	
Sertraline		8	
Paroxetine		7	
Escitalopram		5	
Fluvoxamine		0	
Venlafaxine		3	
Duloxetine		1	
Mirtazapine		0	
Mood stabilizer			
Valproate		25	
Lamotrigine		2	
Lithium		3	
Antipsychotics			
Olanzapine		9	
Quetiapine		16	
Risperidone		2	
Aripiprazole		2	

Abbreviations: HCs, Healthy controls; BDD, Bipolar disorder depression; HAMD, Hamilton depression scale. Values are mean ± standard deviation.
[a] Two-tailed two-sample t-test.
[b] Chi-square test.

3.2. Main effects of diagnosis

A significant lfcd main effect of diagnosis was found (Fig. 1A, Table2). BDD patients showed significantly increased lfcd in the midline cerebelum compared with HCs (Fig. 2).

The significant lrfcd main effect of diagnosis was observed (Fig. 1B, Table2). BDD patients showed significantly increased lrfcd in the left supplementary motor area and right striatum and significantly decreased lrfcd in the bilateral inferior temporal gyrus and left angular gyrus (AG) compared with those in HCs (Fig. 2).

3.3. Interaction effects between the frequency band and diagnosis

A significant lfcd frequency-by-diagnosis interaction effect was observed (Fig. 3A, Table3). BDD patients showed significantly increased lfcd in the left pre-/postcentral gyrus and left fusiform gyrus (FG) in the slow-4 frequency band compared with those in HCs. No significant lfcd region was found in the slow-5 frequency band (Fig. 4).

The significant lrfcd frequency-by-diagnosis interaction effect was observed (Fig. 3B, Table3). BDD patients showed significantly increased lrfcd in the left lingual gyrus (LG) in the slow-4 band whereas significantly decreased in this cluster in the slow-5 compared with that of HCs (Fig. 4).

3.4. Correlation between altered fcd and clinical variables

The increased lfcd in the left FG in the slow-4 band among BDD group was significantly positively correlated with the duration of illness ($r = 0.365$, $p = 0.03$) and number of depressive episodes ($r = 0.434$, $p = 0.007$). The decreased lrfcd within the left AG was significantly

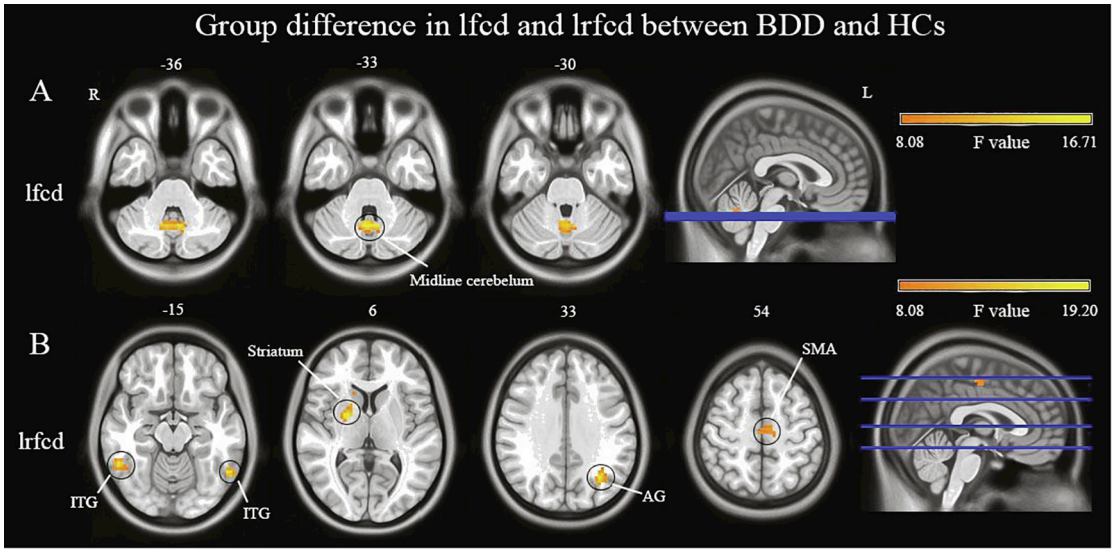

Fig. 1. Main effect of the diagnosis. The results were obtained by two-way ANOVA. Statistical significance level was corrected for multiple comparisons using GRF method with (voxel $p < 0.005$; cluster $p < 0.05$ and the minimum cluster size of the lfcd and lrfcd diagnosis main effect was identified as 38 and 38 voxels, respectively). A. The diagnosis main effect on lfcd. B. The diagnosis main effect on lrfcd. Abbreviations: BDD, Bipolar disorder during depressive episodes; HCs, healthy controls; ITG, inferior temporal gyrus; AG, angular gyrus; SMA, supplementary motor area; L, left; R, right; lfcd, local functional connectivity density; lrfcd, long-range functional connectivity density; ANOVA, analysis of variance.

Table 2
Main effect of the diagnosis.

	Brain areas	Cluster size	L/R	Peak coordinate			*F*-value
		voxels		X	Y	Z	
Group difference in lfcd revealed by a two-way ANOVA							
Cluster 1	Midline cerebelum	92	R	3	−60	−33	16.77
Group difference in lrfcd revealed by a two-way ANOVA							
Cluster 1	Inferior temporal gyrus	39	R	54	−48	−15	17.34
Cluster 2	Inferior temporal gyrus	78	L	−57	−57	−15	17.08
Cluster 3	Striatum	97	R	21	0	6	19.28
Cluster 4	Angural gyrus	41	L	−33	−63	33	17.43
Cluster 5	Supplementary motor area	57	L	−12	−18	54	11.01

Statistical significance level was corrected for multiple comparisons using GRF method with (voxel $p < 0.005$; cluster $p < 0.05$ and the minimum cluster size of the lfcd and lrfcd diagnosis main effect was identified as 38 and 38 voxels, respectively). The peak coordinate was defined in MNI space. Abbreviations: L, left; R, right; lfcd, local functional connectivity density; lrfcd, long-range functional connectivity density; GRF, Gaussian random field; ANOVA, analysis of variance; MNI, Montreal Neurological Institute.

negatively correlated with the HAMD scores ($r = -0.33$, $p = 0.04$) (Fig. 5).

4. Discussion

This study used the voxel-level fcd method to investigate the FC pattern alterations among BDD patients at two frequency bands (i.e., slow-5 and slow-4). Our main findings were as follows: 1) BDD patients showed aberrant functional communication in the DMN, SMN, and subcortical and limbic modulating regions (striatum and midline cerebelum). 2) BDD patients showed increased functional communication in the slow-4 band and decreased exhibited functional communication in the slow-5 band in the sensory system regions. 3) These fcd alterations were correlated with the clinical variables.

4.1. Group difference in fcd between BDD and HCs

Lrfcd captures long distance brain communication which demands high metabolic and time costs (Tomasi and Volkow, 2017). The disrupted long-range information interaction is associated with the loss of brain network efficiency and may lead to abnormal cognition and clinical manifestation in psychiatry disorders (Cui et al., 2017; Wang et al., 2017b; Zhang et al., 2016, 2017). In the present study, we found abnormal lrfcd in the DMN and SMN in BDD patients. DMN is implicated in self-related cognitive activity, while SMN is sensitive to extrinsic environment stimuli, and the disbalance between DMN and SMN activity is related to rumination and psychomotor behavior (Martino et al., 2016). A recent physiological research concluded that alterations in neurotransmitters signaling may favor these correspondent functional reorganization of DMN and SMN, manifesting in distinct psychopathological states in BD (Conio et al., 2020). On the basis of the aforementioned findings, abnormal lrfcd patterns in the DMN and SMN probably related to clinical symptoms of BDD, such as cognitive impairment and psychomotor retardation.

Furthermore, we observed increased lfcd and lrfcd in the midline cerebellum and striatum, respectively, in BDD patients. Previous study found that the midline cerebellum was strongly interconnected with limbic brain regions (Schmahmann and Sherman, 1998) and reported the midline cerebellum atrophy in BD (Strakowski et al., 2005b). The structural abnormalities and increased cerebral blood flow value of the striatum among BDD patients have been reported (He et al., 2019). Also, previous study found that specific injury to the right caudate head

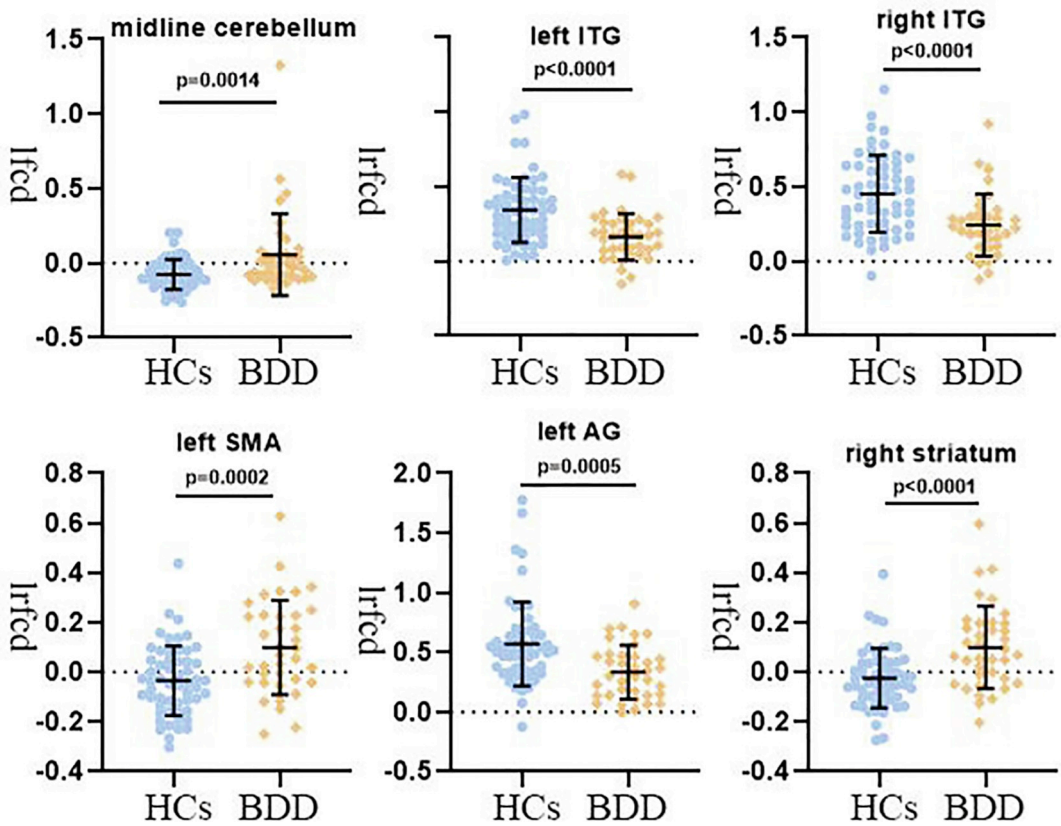

Fig. 2. Simple effect of the diagnosis on lfcd and lrfcd. Abbreviations: BDD, Bipolar disorder during depressive episodes; HCs, healthy controls; ITG, inferior temporal gyrus; SMA, supplementary motor area; AG, angular gyrus; lfcd, local functional connectivity density; lrfcd, long-range functional connectivity density.

may precipitate mood cycling, similar to that observed in BD (Starkstein et al., 1991). Neuroanatomical and functional imaging studies support a model of BD concerning the brain dysfunction of patients within the prefrontal–striatal–thalamic circuits and the associated limbic modulating regions (amygdala, midline cerebellum) (Strakowski et al., 2005). The current results might suggest the disrupted modulation function of the prefrontal cortex to the subcortical and limbic modulating regions in BDD and may be correlated with the dysregulation of mood in such disease.

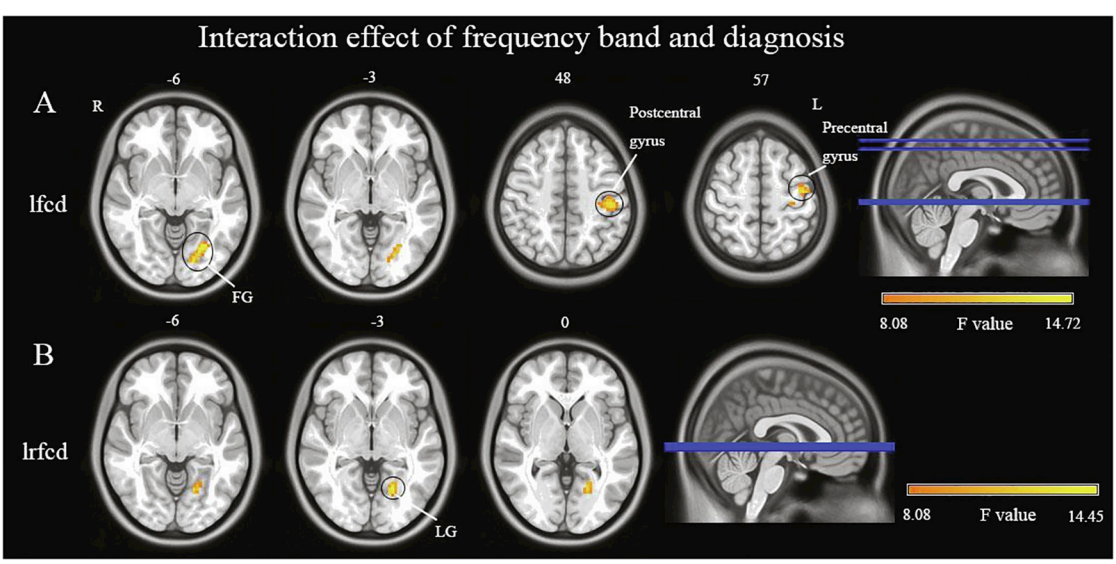

Fig. 3. Interaction effect of the frequency band and diagnosis. The results were obtained by two-way ANOVA. Statistical significance level was corrected for multiple comparisons using GRF method with (voxel $p < 0.005$; cluster $p < 0.05$ and the minimum cluster size of the lfcd and lrfcd interaction effect was identified as 33 and 29 voxels, respectively). A. The interaction between the frequency band and diagnosis on lfcd. B. The interaction between the frequency band and diagnosis on lrfcd. Abbreviations: FG, fusiform gyrus; LG, lingual gyrus; L, left; R, right; lfcd, local functional connectivity density; lrfcd, long-range functional connectivity density; ANOVA, analysis of variance.

Table 3
Interaction effect between the frequency band and diagnosis.

	Brain areas	Cluster size	L/R	Peak coordinate			*F*-value
		voxels		X	Y	Z	
Interaction effect between the frequency band and diagnosis on lfcd							
Cluster 1	Fusiform gyrus	54	L	−27	−66	−6	14.78
Cluster 2	Pre-/Postcentral gyrus	121	L	−45	−24	48	13.47
Interaction effect between the frequency band and diagnosis on lrfcd							
Cluster 1	Lingual gyrus	50	L	−21	−63	−3	14.50

Statistical significance level was corrected for multiple comparisons using GRF method with (voxel $p < 0.005$; cluster $p < 0.05$ and the minimum cluster size of the lfcd and lrfcd interaction effect was identified as 33 and 29 voxels, respectively). The peak coordinate was defined in MNI space. Abbreviations: L, left; R, right; lfcd, local functional connectivity density; lrfcd, long-range functional connectivity density; GRF, Gaussian random field; ANOVA, analysis of variance; MNI, Montreal Neurological Institute.

4.2. Frequency-dependent changes in fcd in BDD

The increased lfcd and lrfcd of the sensory system regions in the slow-4 band were found in BDD patients compared with those in HCs. The abnormalities in white matter in left-sided temporo-occipitoparietal cortical regions is related to the pathology mechanism of BDD (Versace et al., 2010) and implicated abnormal face-emotion processing in BD (Stoddard et al., 2016). Additionally, abnormally elevated medial occipital activity was also found in BDD patients during attention and executive function-related tasks (Strakowski et al., 2005a). The increased connectivity in the sensory system in BDD may signify changes in face-emotional processing and dysfunction in cognition in depressed state. Moreover, a prior study has reported that the sensory system displayed a considerable spatial extent in the slow-4 band than that of slow-5 (Gohel and Biswal, 2014). Our result expands the results of these previous studies by showing that the functional communication in sensory system regions were increased in the slow-4 band in BDD patients. This finding offered a new framework for the better understanding of BDD from the voxel-wise FC in frequency perspective.

The decreased lrfcd in the LG in the slow-5 band was found in BDD patients compared with HCs. LG is also known as the medial occipitotemporal gyrus, which located below the calcarine fissure, posterior to the parahippocampal gyrus. A prior study found that abnormal activation in the LG and prefrontal regions were associated with episodic memory impairments of BD patients (Oertel-KnoeChel et al., 2014). Another fMRI study observed abnormal connectivity in prefrontal and LG regions in BDD patients (Wang et al., 2016). Moreover, several previous studies in HCs found that the prefrontal cortex exhibited higher functional activity in the slow-5 band (Han et al., 2011, Zuo et al., 2010). On the basis of the aforementioned findings, the current result might suggest abnormal regulation of the prefrontal cortex to LG. However, consider the *p* value of this decreased lrfcd in the slow-5 in BDD compared with that of HCs is marginal significant, the understanding of this result should be cautious.

4.3. Correlation between altered fcd and clinical variables

The decreased lrfcd in the left AG was negatively associated with HAMD scores of the BDD group. A previous research found that decreased FC of the AG in BDD but not in bipolar patients in remission (Lv et al., 2016). Our result provide further evidence of the dysfunction of the AG in BDD. Moreover, we found the frequency-specific increased lfcd in FG was positively correlated with the duration of illness and number of depression episodes of BDD. The greater FG activity to emotional faces were associated with greater future irritability (Karim and Perlman, 2017). Additionally, abnormal activity of the FG has been reported in BD using facial affect recognition tasks (Strakowski et al., 2004). A previous longitudinal study found that BD patients showed a larger gray matter density decline in the FG than HCs (Moorhead et al., 2007). Our result expands previous findings by showing that the FCs of FG in slow-4 in BDD patients may exhibit progressive properties.

5. Limitation

The current study has several limitations. First, almost all patients were taking medications at the time of the scan. Although no significant correlation between the aberrant fcd and the total medication load was found, medication treatment may have potential effects on our neuroimaging findings (Pang et al., 2018). Second, several studies found that the different mood states, such as the manic and depressive states have different effects on functional systems of BD (Martino et al., 2016). Future studies on patients in different states are expected to clarify this

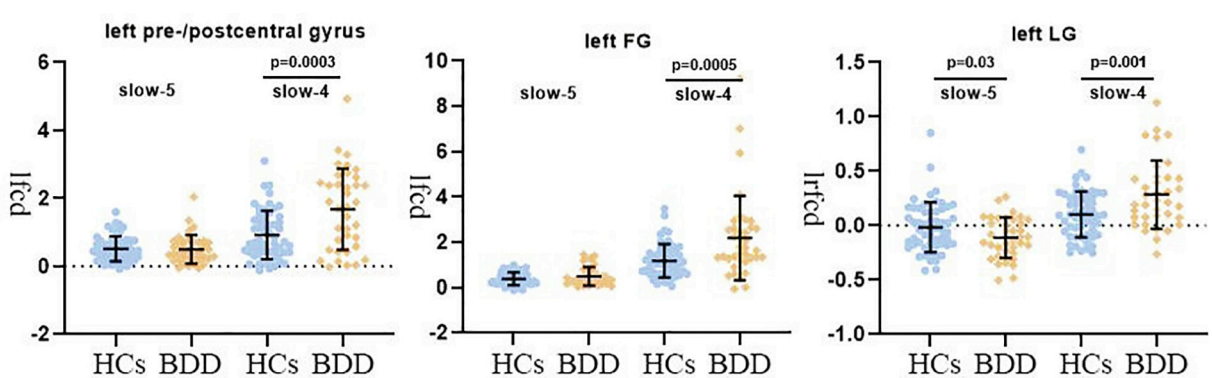

Fig. 4. Simple effect of the interaction effect between frequency band and diagnosis on lfcd and lrfcd. Abbreviations: BDD, Bipolar disorder during depressive episodes; HCs, healthy controls; FG, fusiform gyrus; lfcd, LG, lingual gyrus; local functional connectivity density; lrfcd, long-range functional connectivity density.

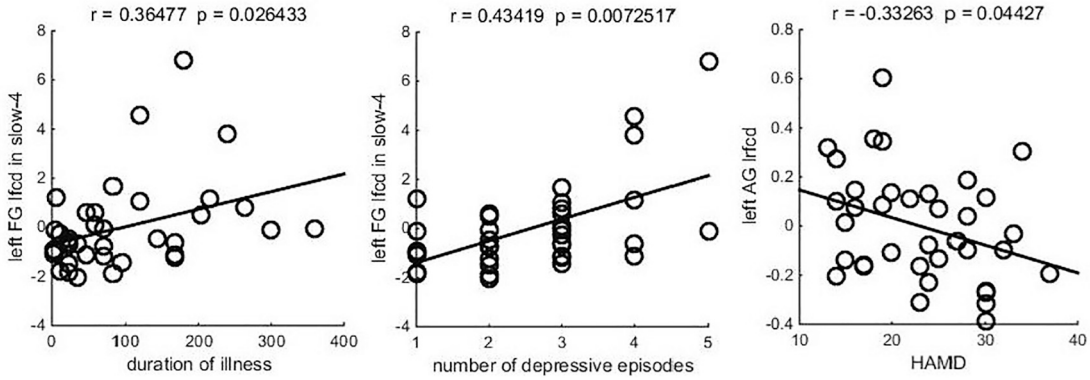

Fig. 5. Correlation with the clinic variables. Correlation between regions showing significant main and interaction effect and clinical variabled with medication as a covariate in patients with BDD ($p < 0.05$, uncorrected). Abbreviations: BDD, Bipolar disorder during depressive episodes; FG, fusiform gyrus; AG, angular gyrus; lfcd, local functional connectivity density; lrfcd, long-range functional connectivity density; HAMD, Hamilton depression scale.

issue. Third, multimodal neuroimaging data can provide relatively comprehensive information about the pathomechanisms of psychiatric disorders. Future studies are expected to combine the structural and functional neuroimaging data (Li et al., 2016), multi-frequency bands, and pattern recognition analyses to provide further information about BDD patients.

6. Conclusion

We investigated the changes in FC in BDD patients at specific frequency bands. Our results scored the DMN, SMN, and subcortical and limbic modulating regions (striatum and midline cerebelum) dysfunction in BDD. The frequency-specific FC pattern dysfunction in the sensory system may imply abnormal emotional processing and aberrant cognitive function in BDD. In addition, the abnormal FC pattern in FG was correlated with clinical progression whereas the FC pattern in the AG was correlated with depressive symptom severity. These findings suggested the importance of investigating the frequency-dependent FC patterns to improve our understanding of the pathomechanism in BDD.

Ethical statement

All participants were informed about the procedures and details of the study and provided written informed consent. This study was approved by the research ethical committee of the University of Electronic Science and Technology of China, listed on Clinical-Trials.gov (Registration Number: NCT02888509)

Author contribution

Authors Yang Yang, Qian Cui, and Huafu Chen designed the study. Qian Cui and Zongling He interviewed all patients using the DSM–IV. Yang Yang, Qin Tang, Ailing Xie, Jing Huang, Di Li, Ting Lei, Xiaonan Guo, and Yifeng Wang participated in the data collection. Yang Yang and Yajing Pang analyzed the data. Yuyan Chen, Shaoqiang Han, and Qian Cui supervised the data analysis. Yang Yang and Yajing Pang wrote the first draft of the manuscript. Qian Cui, Xiaonan Guo, AHMED AMEEN FATEH, Fengmei Lu, and Zongling He gave their critical revision of the manuscript. All authors contributed to and have approved the final manuscript.

Funding source

This study was supported by the Key Project of Research and Development of Ministry of Science and Technology (2018AAA0100705), the Natural Science Foundation of China (61533006, U1808204, 81771919), the Scientific research project of Sichuan Medical Association (S15012), the Youth Innovation Project of Sichuan Provincial Medical Association (Q14014), and the China Postdoctoral Science Foundation Grant (2019M653383).

Declaration of Competing Interest

The authors declare that they have no known competing financial interests or personal relationships that could have appeared to influence the work reported in this paper

Acknowledgement

We thank all subjects participate in this study.

Appendix A. Supplementary data

Supplementary data to this article can be found online at https://doi.org/10.1016/j.pnpbp.2020.110026.

References

Almeida, J.R., Akkal, D., Hassel, S., Travis, M.J., Banihashemi, L., Kerr, N., et al., 2009. Reduced gray matter volume in ventral prefrontal cortex but not amygdala in bipolar disorder: significant effects of gender and trait anxiety. Psychiatry Res. 171, 54–68.
Ambrosi, E., Arciniegas, D.B., Madan, A., Curtis, K.N., Patriquin, M.A., Jorge, R.E., et al., 2017. Insula and amygdala resting-state functional connectivity differentiate bipolar from unipolar depression. Acta Psychiatr. Scand. 136, 129–139.
Amelia, V., 2008. Elevated left and reduced right orbitomedial prefrontal fractional anisotropy in adults with bipolar disorder revealed by tract-based spatial statistics. Arch. Gen. Psychiatry 9, 1041–1052.
Anand, A., Li, Y., Wang, Y., Lowe, M.J., Dzemidzic, M., 2009. Resting state corticolimbic connectivity abnormalities in unmedicated bipolar disorder and unipolar depression. Psychiatry Res.: Neuroimaging 171, 189–198.
Buzsáki, G., Draguhn, A., 2004. Neuronal oscillations in cortical networks. Science 304, 1926–1929.
Conio, B., Martino, M., Magioncalda, P., Escelsior, A., Inglese, M., Amore, M., et al., 2020. Opposite effects of dopamine and serotonin on resting-state networks: review and implications for psychiatric disorders. Mol. Psychiatry 25, 82–93.
Cordes, D., Haughton, V.M., Arfanakis, K., Carew, J.D., Turski, P.A., Moritz, C.H., et al., 2001. Frequencies contributing to functional connectivity in the cerebral cortex in "resting-state" data. AJNR Am. J. Neuroradiol. 22, 1326–1333.
Cui, Q., Vanman, E.J., Long, Z., Pang, Y., Chen, Y., Wang, Y., et al., 2017. Social anxiety disorder exhibit impaired networks involved in self and theory of mind processing. Soc. Cogn. Affect. Neurosci. 12, 1284–1295.
Friston, K.J., Williams, S., Howard, R., Frackowiak, R.S.J., Turner, R., 1996. Movement-related effects in fMRI time-series. Magn. Reson. Med. 35, 346–355.
Gohel, S.R., Biswal, B.B., 2014. Functional integration between brain regions at rest occurs in multiple-frequency bands. Brain Connect. 5, 23–34.
Goya-Maldonado, R., Brodmann, K., Keil, M., Trost, S., Dechent, P., Gruber, O., 2016. Differentiating unipolar and bipolar depression by alterations in large-scale brain networks. Hum. Brain Mapp. 37, 808–818.
Grande, Iria, Berk, Michael, Birmaher, Boris, et al., 2016. Bipolar disorder. Lancet 387, 1561–1572.
Guo, X., Duan, X., Chen, H., He, C., Xiao, J., Han, S., et al., 2020. Altered inter- and intrahemispheric functional connectivity dynamics in autistic children. Hum. Brain

Mapp. 41, 419–428.
Han, Y., Wang, J., Zhao, Z., Min, B., Lu, J., Li, K., et al., 2011. Frequency-dependent changes in the amplitude of low-frequency fluctuations in amnestic mild cognitive impairment: a resting-state fMRI study. NeuroImage. 55, 287–295.
He, Z., Sheng, W., Lu, F., Long, Z., Han, S., Pang, Y., et al., 2019. Altered resting-state cerebral blood flow and functional connectivity of striatum in bipolar disorder and major depressive disorder. Prog. Neuro-Psychopharmacol. Biol. Psychiatry 90, 177–185.
He, H., Yu, Q., Du, Y., Vergara, V., Victor, T.A., Drevets, W.C., et al., 2016. Resting-state functional network connectivity in prefrontal regions differs between unmedicated patients with bipolar and major depressive disorders. J. Affect. Disord. 190, 483–493.
John, M.D., 2004. Dose response and dose equivalence of antipsychotics. J. Clin. Psychopharmacol. 2, 192–208.
Karim, H.T., Perlman, S.B., 2017. Neurodevelopmental maturation as a function of irritable temperament. Hum. Brain Mapp. 38, 5307–5321.
Li, R., Liao, W., Li, Y., Yu, Y., Zhang, Z., Lu, G., et al., 2016. Disrupted structural and functional rich club organization of the brain connectome in patients with generalized tonic-clonic seizure. Hum. Brain Mapp. 37, 4487–4499.
Lv, D., Lin, W., Xue, Z., Pu, W., Yang, Q., Huang, X., et al., 2016. Decreased functional connectivity in the language regions in bipolar patients during depressive episodes but not remission. J. Affect. Disord S0165032715311137.
Magioncalda, P., Martino, M., Conio, B., Escelsior, A., Piaggio, N., Presta, A., et al., 2015. Functional connectivity and neuronal variability of resting state activity in bipolar disorder—reduction and decoupling in anterior cortical midline structures. Hum. Brain Mapp. 36, 666–682.
Martino, M., Magioncalda, P., Huang, Z., Conio, B., Piaggio, N., Duncan, N.W., et al., 2016. Contrasting variability patterns in the default mode and sensorimotor networks balance in bipolar depression and mania. Proc. Natl. Acad. Sci. 113, 4824–4829.
Mitchell, P.B., Goodwin, G.M., Johnson, G.F., Hirschfeld, R.M., 2010. Diagnostic guidelines for bipolar depression: a probabilistic approach. Bipolar Disord. 10, 144–152.
Mitchell, P.B., Malhi, G.S., 2004. Bipolar depression: phenomenological overview and clinical characteristics. Bipolar Disord. 6, 530–539.
Moorhead, T.W.J., McKirdy, J., Sussmann, J.E.D., Hall, J., Lawrie, S.M., Johnstone, E.C., et al., 2007. Progressive gray matter loss in patients with bipolar disorder. Biol. Psychiatry 62, 894–900.
Oertel-KnoeChel, V., Reinke, B., Feddern, R., Knake, A., KönChel, C., Prvulovic, D., et al., 2014. Episodic memory impairments in bipolar disorder are associated with functional and structural brain changes. Bipolar Disord. 16, 830–845.
Pang, Y., Chen, H., Wang, Y., Long, Z., He, Z., Zhang, H., et al., 2018. Transdiagnostic and diagnosis-specific dynamic functional connectivity anchored in the right anterior insula in major depressive disorder and bipolar depression. Prog. Neuro-Psychopharmacol. Biol. Psychiatry 85, 7–15.
Perry, A., Roberts, G., Mitchell, P.B., Breakspear, M., 2018. Connectomics of bipolar disorder: a critical review, and evidence for dynamic instabilities within interoceptive networks. Mol. Psychiatry 24, 1296–1318.
Power, J.D., Barnes, K.A., Snyder, A.Z., Schlaggar, B.L., Petersen, S.E., 2012. Spurious but systematic correlations in functional connectivity MRI networks arise from subject motion. Neuroimage. 59, 2142–2154.
Sackeim, H., 2001. The definition and meaning of treatment-resistant depression. J. Clin. Psychiatry (Suppl 16), 10–17.
Satterthwaite, T.D., Kable, J.W., Vandekar, L., Katchmar, N., Bassett, D.S., Baldassano, C.F., et al., 2015. Common and dissociable dysfunction of the reward system in bipolar and unipolar depression. Neuropsychopharmacology 40, 2258–2268.
Schmahmann, J.D., Sherman, J.C., 1998. The cerebellar cognitive affective syndrome. Brain 121, 561–579.
Shuixia, G., Lena, P., Bo, Y., Zhening, L., Zhimin, X., Jianfeng, F., 2014. Anatomical distance affects functional connectivity in patients with schizophrenia and their siblings. Schizophr. Bull. 40, 449–459.
Smith, S.M., Fox, P.T., Miller, K.L., Glahn, D.C., Fox, P.M., Mackay, C.E., et al., 2009. Correspondence of the brain's functional architecture during activation and rest. PNAS 106, 13040–13045.
Spielberg, J.M., Beall, E.B., Hulvershorn, L.A., Altinay, M., Karne, H., Anand, A., 2016. Resting state brain network disturbances related to hypomania and depression in medication-free bipolar disorder. Neuropsychopharmacology 41, 3016–3024.
Starkstein, S.E., Fedoroff, P., Berthier, M.L., Robinson, R.G., 1991. Manic-depressive and pure manic states after brain lesions. Biol. Psychiatry 29, 149–158.
Stoddard, J., Gotts, S.J., Brotman, M.A., Lever, S., Hsu, D., Zarate, C., et al., 2016. Aberrant intrinsic functional connectivity within and between corticostriatal and temporal–parietal networks in adults and youth with bipolar disorder. Psychol. Med. 46, 1509–1522.
Strakowski, S.M., Adler, C.M., Holland, S.K., Mills, N., DelBello, M.P., 2004. A preliminary fMRI study of sustained attention in euthymic, unmedicated bipolar disorder. Neuropsychopharmacology 29, 1734–1740.
Strakowski, S., Delbello, M., Adler, C., 2005. The functional neuroanatomy of bipolar disorder: a review of neuroimaging findings. Mol. Psychiatry 10, 105–116.
Tomasi, D., Volkow, N.D., 2010. Functional connectivity density mapping. PNAS 107, 9885–9890.
Tomasi, D., Volkow, N.D., 2012. Resting functional connectivity of language networks: characterization and reproducibility. Mol. Psychiatry 17, 841–854.
Tomasi, D., Volkow, N.D., 2017. Reduced local and increased long-range functional connectivity of the thalamus in autism spectrum disorder. Cereb. Cortex 29, 573–585.
Versace, A., Almeida, J.R.C., Quevedo, K., Thompson, W.K., Terwilliger, R.A., Hassel, S., et al., 2010. Right orbitofrontal corticolimbic and left corticocortical white matter connectivity differentiate bipolar and unipolar depression. Biol. Psychiatry 68, 560–567.
Wang, X., Zhang, Y., Long, Z., Zheng, J., Zhang, Y., Han, S., et al., 2017a. Frequency-specific alteration of functional connectivity density in antipsychotic-naive adolescents with early-onset schizophrenia. J. Psychiatr. Res. 95, 68–75.
Wang, Y., Zhong, S., Jia, Y., Sun, Y., Wang, B., Liu, T., et al., 2016. Disrupted resting-state functional connectivity in nonmedicated bipolar disorder. Radiology 280, 529–536.
Wang, Y., Wang, J., Jia, Y., Zhong, S., Niu, M., Sun, Y., et al., 2017b. Shared and specific intrinsic functional connectivity patterns in unmedicated bipolar disorder and major depressive disorder. Sci. Rep. 7, 3570.
Zhang, Z., Liao, M., Yao, Z., Hu, B., Xie, Y., Zheng, W., et al., 2017. Frequency-specific functional connectivity density as an effective biomarker for adolescent generalized anxiety disorder. Front. Hum. Neurosci. 11.
Zhang, Y., Xie, B., Chen, H., Li, M., Liu, F., Chen, H., 2016. Abnormal functional connectivity density in post-traumatic stress disorder. Brain Topogr. 29, 405–411.
Zuo, X.N., Martino, A.D., Kelly, C., Shehzad, Z.E., Gee, D.G., Klein, D.F., et al., 2010. The oscillating brain: complex and reliable. Neuroimage 49, 1432–1445.